The Dark Horse of Evaluating Long-Term Field Performance—Data Filtering

Dirk C. Jordan and Sarah R. Kurtz

***Abstract*—This paper addresses an issue of long-term performance that has seen relatively little attention in the industry, yet we will show that it can be of vital importance, not only for obvious financial reasons but, technically, because of its linkage to field failure as well. We will discuss how different data filtering on one particular system can lead to a variety of different degradation rates compared with indoor measurements and how it may change the field failure interpretation for a single module. A method based on the variation of the uncertainty in the determined degradation rates is proposed to aid the data filtering process when no baseline measurements exist. Finally, based on this experience, we propose a set of guidelines as a basis for a standardized approach to long-term performance assessment.**

***Index Terms*—Data filtering, degradation rate, field failure, field performance, performance, photovoltaics (PVs).**

I. Introduction

WORLDWIDE photovoltaic (PV) installations represent investments that can be already measured as a percentage of gross domestic products of respective countries. At this magnitude, it is critical to all stakeholders to determine and predict long-term performance accurately. Fig. 1 shows a histogram of historical degradation rates (R_d) partitioned by method of measurement with an extreme value distribution [1]. A significant number of degradation rates—a negative degradation rate is defined in this paper as a performance loss—have been determined using continuous performance data. Contrary to current-voltage (IV) data that are typically taken under carefully controlled conditions, continuous data need to be reduced for performance evaluation. The process of preferentially choosing a subset (data filtering), such as data for sunny-only days, can increase the accuracy of the long-term analysis, as it has been shown using the photovoltaics for utility scale applications (PVUSA) methodology and is also incorporated in the standard ASTM E2848–11 [2], [3]. Furthermore, a combination of binning, data filtering, and data only from the same time period of the year has been shown to reduce degradation rate uncertainty [4], [5]. However, the filtering process may not only affect the uncertainty but the degradation rate itself as well. In some cases, differences in degradation rates reflect a true difference, as when a module decreases in low-light performance relatively faster than at full-sun conditions, but in most cases, the difference reflects the variability of the data. As there are different metrics and filtering methods in use, a standard approach would be useful such that two analysts derive the same result for the same dataset. To this end, we have determined degradation rates for a mono-crystalline Si (mono-Si) system for a variety of different performance metrics and filtering conditions on the same dataset, as we discuss in the first section. The second part examines the impact of data filtering on the salient IV parameters—maximum power $(P_{\max})$, short-circuit current $(I_{\rm sc})$, open-circuit voltage $(V_{\rm oc})$, and fill factor (FF)—on a mono-Si module collected automatically over the last 17 years and establishes the link with field failure. Finally, we introduce a filtering optimization based on uncertainty minimization and summarize our overall findings in a set of guidelines that may be utilized in the development of a standard approach to long-term performance assessment.

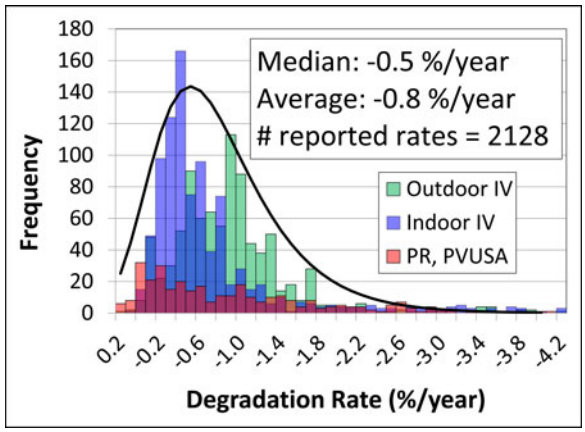

Fig. 1. Histogram of historical degradation rates, and itemized by method of measurement, with an extreme value distribution fit.

II. System Data

Fig. 2 shows the degradation rate for a 1.4-kW-mono-Si system fielded for almost ten years at NREL as a function of different metrics and filtering conditions. The system consists of five modules, installed in portrait orientation in one string. The array was mounted at a latitude tilt of 40° facing due south and was utility grid tied through an SMA Sunnyboy inverter with its own maximum-power-point-tracking algorithm [6]. The metrics used for the determination of the degradation rates are a temperature-corrected ratio of dc power over the plane-of-array irradiance (DC/$G_{\rm POA}$) [7], the performance ratio (PR) utilizing

Manuscript received June 10, 2013; revised September 3, 2013; accepted September 8, 2013. Date of publication October 3, 2013; date of current version December 16, 2013. This work was supported by the U.S. Department of Energy under Contract DE-AC36–08-GO28308 with the National Renewable Energy Laboratory.

The authors are with the National Renewable Energy Laboratory, Golden, CO 80401 USA (e-mail: dirk.jordan@nrel.gov; Sarah.Kurtz@nrel.gov).

Color versions of one or more of the figures in this paper are available online at http://ieeexplore.ieee.org.

Digital Object Identifier 10.1109/JPHOTOV.2013.2282741

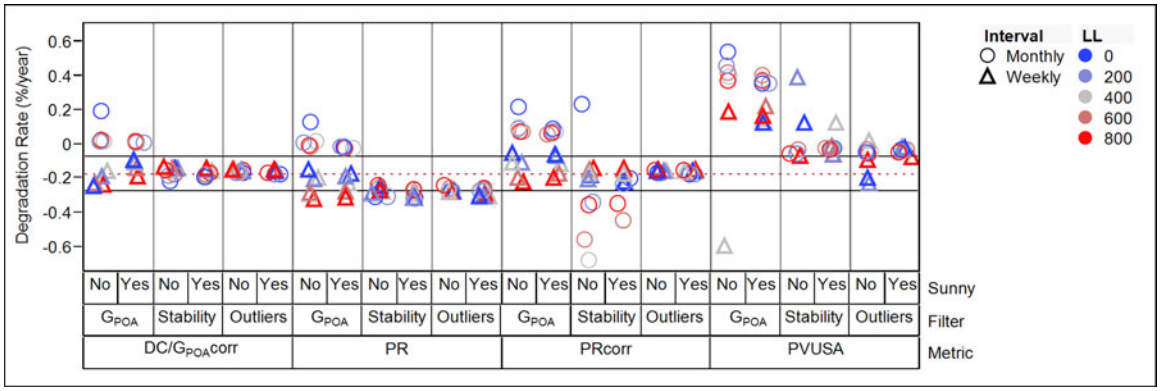

Fig. 2. Degradation rates for a mono-crystalline Si system as a function of different metrics and filtering conditions. Degradation rate determined by indoor IV measurements (red-dashed line) and a 0.1%/year interval (black lines) are given as guide to the eye.

nameplate rating with and without temperature correction [8], and lastly the regression PVUSA method. [9]

The analysis is based on dc power data to minimize inverter effects; however, a comparable analysis could be applied to ac power data. Manufacturer temperature coefficients were used for the temperature-corrected metrics to adjust to 45 °C module temperature. Two remaining effects, spectral and angle-of-incidence corrections have not been applied and may contribute to some residual variability. The time interval in which the performance metric is evaluated is given in monthly and weekly increments. The upper limit for G_{POA} was fixed at 1200 W/m^2, which, for the Colorado climate, is a good way to reduce the effect of cloud brightening. The lower limit (LL) was varied between 0 and 800 W/m^2. Two filters were applied in addition to the G_{POA} filtering and are denoted by "stability" and "outliers." The aptly named stability filter eliminates data points when the G_{POA} changes more than 20 W/m^2/min and the module temperature more than 1 °C/min. In addition to the stability screening, the outlier filter uses the difference between module and ambient temperature and the ratio DC/G_{POA} to eliminate snow days and partial-shading conditions, as illustrated more clearly in Section IV. Furthermore, the data for sunny days were selected by filtering for clearness index > 0.5. (Clearness index is the ratio of measured global irradiance over the extraterrestrial beam irradiance on a similarly tilted surface [10].)

The calculated degradation rates can be compared with rates obtained from indoor IV measurements taken before field deployment and after six years of exposure (dashed line). The temperature-corrected DC/G_{POA} ratio is in excellent agreement with the indoor IV data when all three data filters are applied. The PR shows good precision but indicates some deviation from the indoor IV for the same filtering. The accuracy, the deviation from the indoor measurements, and precision, i.e., the scatter of the data in each category, is improved if the PR is temperature corrected. The PVUSA methodology shows fairly large scatter, especially when using weekly increments. It is also the metric that benefits the most by using only sunny days, which has been previously shown [2].

Seasonal fluctuations can have significant impact on the determined degradation rates not only by increasing the uncertainties, but by leading to systematic deviations, particularly for non-

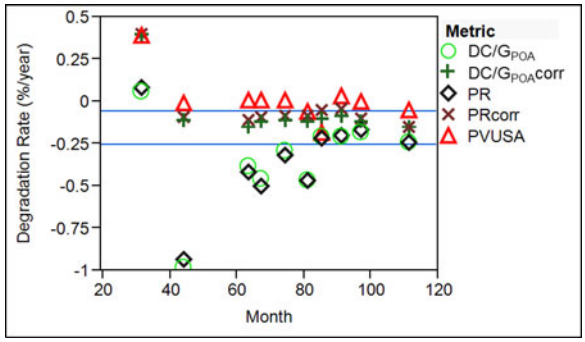

Fig. 3. Degradation rates as a function of field exposure for different metrics using weekly increments, as described in the text.

temperature metrics. Fig. 3 shows degradation rates determined when the "outlier" filter was used as a function of field exposure using weekly increments. In addition to the metrics used in Fig. 2, the uncorrected ratio DC/G_{POA} was used. A 0.1%/year interval around the rate determined from the indoor IV data is indicated by the solid blue lines. The temperature-corrected metrics show minimal fluctuations and are in excellent agreement even for three and half years of field data. The uncorrected metrics, both DC/G_{POA} and PR show significant fluctuations depending on the time of the year in addition to more systematic bias. The regression approach, i.e., PVUSA, also shows a dependence on seasonality and a systematic bias for almost the entire field exposure.

III. Individual Module

Fig. 4 illustrates the quandary of data filtering for an individual module. The 75-W mono-Si module, that is different from the ones comprising the system of Section II, was mounted on the performance and energy rating testbed which has been previously described in detail [11]. IV parameters collected automatically over the last 17 years in 15-min increments were investigated. The degradation rates for the salient IV parameters—maximum power (P_{max}), short-circuit current (I_{sc}), open-circuit voltage (V_{oc}), fill factor (FF)—are shown as a function of a stability filter. The upper G_{POA} limit was fixed at 1200 W/m^2, and two different lower G_{POA} limits were used.

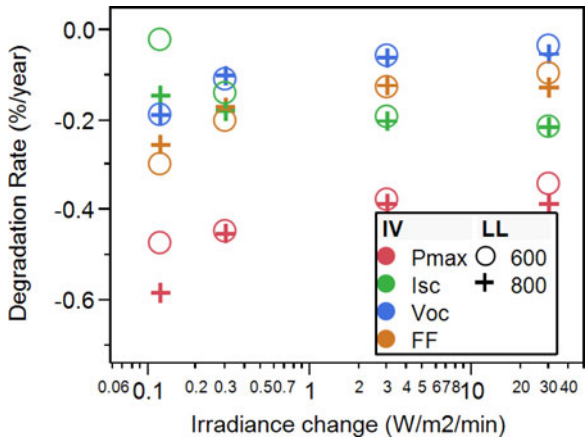

Fig. 4. Degradation rates of IV parameters for mono-Si module. The G_{POA} upper limit was fixed at 1200 W/m^2, and two different lower limits were used (LL).

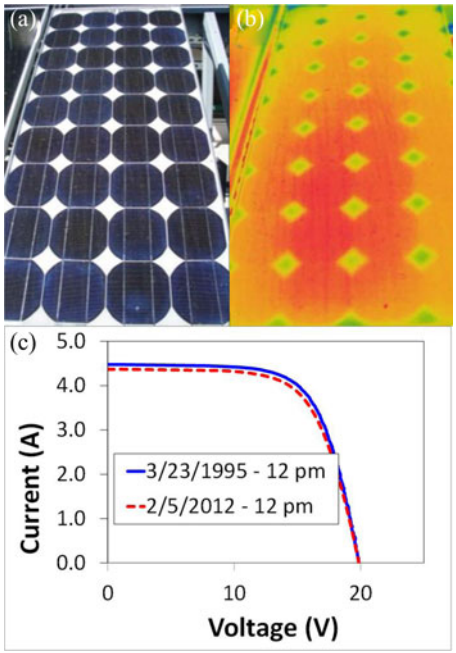

Fig. 5. (a) Optical image, (b) infrared image of the mono-Si module, and (c) irradiance- and temperature-corrected *I–V* curves, before and after 17 years of field exposure.

Significant changes can be discerned, as the irradiance stability is tightened. The lowest points in the figure show a degradation that is mostly dominated by FF loss, while a less-stringent filter on G_{POA} change shows a tendency toward I_{sc} loss. The difference is exacerbated for a lower G_{POA} limit. The following question arises: Is this module suffering more from I_{sc} or FF loss?

Fig. 5 shows (a) an optical and (b) infrared image of the individual module and (c) a pair of irradiance- and temperature-corrected IV curves according to IEC 60891 before and after 17 years of field exposure. No evidence of shunting or series resistance increase was observed (as is typically associated with FF loss). In addition, the IR image revealed no hot spots. The only visual degradation observed was some permanent soiling and encapsulant discoloration.

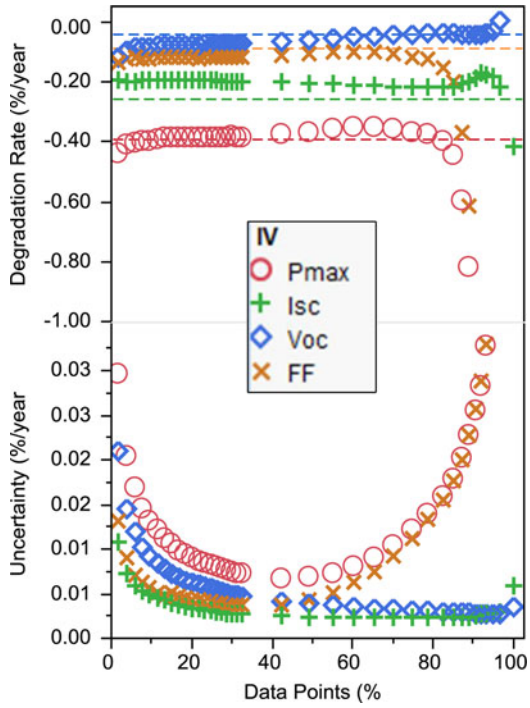

Fig. 6. Degradation rates and uncertainty as a function of percentage of data points left in the dataset. Rates determined from indoor IV measurements are indicated by dashed lines.

In Fig. 6, we provide additional indoor IV characterization results (dashed lines) that show a more I_{sc}-dominated loss historically attributed to delamination, discoloration, and cracked individual cells, while a smaller percentage can be attributed to light-induced degradation and soiling [12]–[14]. Additionally, Fig. 6 may also hold the key for assessing the situation more accurately when no indoor IV measurements are available.

Degradation rates (top panel) and calculated uncertainties, i.e., Type A, (bottom panel) are shown as a function of the percentage of data points left in the dataset for each IV parameter. The uncertainty utilized in this paper is obtained by statistical methods only and does not include measurement uncertainty [15]. When no data filtering is done, the uncertainty is fairly high. As the filtering increases around the median of the filtering parameter, so does the "cleanliness" of the dataset; meanwhile, the uncertainty decreases. If the filtering continues to tighten, a greater and greater number of data points are removed from the dataset, ultimately resulting in an increase of the uncertainty again. Between those two extremes is a region where the uncertainty is relatively constant. In that regime, the determined degradation rates are in good agreement with the rates determined from indoor characterization. Thus, the uncertainty curve can be used when filtering changes to determine the most likely regime for degradation rate determination.

IV. Outlier and Stability Filter

In the previous two sections, we showed the impact that outlier and stability filters of various strengths can have on system and module evaluation. The following section illustrates the importance of these filters in combination with the uncertainty

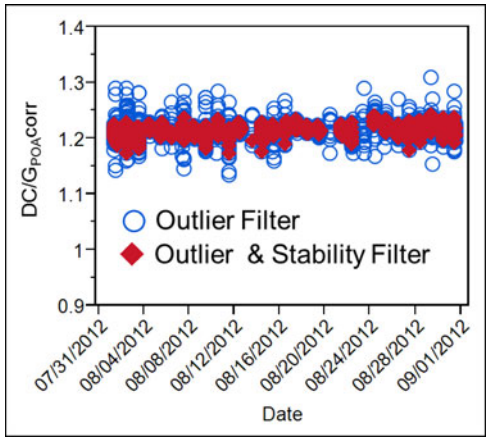

Fig. 7. Ratio dc power over POA irradiance using only an outlier filter (blue circles) and an additional stability filter (red triangles) for the month of August 2012.

minimization for common long-term field performance evaluation problems, extremely variable days, shading, and snow. Fig. 7 illustrates the impact of using only an outlier filter and an additional stability filter on the temperature-corrected DC/G_{POA} ratio for the month of August 2012. This month showed a particular large number of variable days. It can be seen that the outlier filter removes extreme outliers, however, the addition of the stability filter leads to a much improved signal-to-noise ratio.

Furthermore, the utility of these filters is demonstrated on two frequent problems in evaluating field data, losses due shading and snow coverage (in applicable climates). When field data are used to compare to a model it is imperative to identify those loss situations and incorporate them into the modeling. For long-term performance assessment, these situations can lead to an increase in the uncertainty and should be removed. The filtering method utilizing the degradation rate uncertainty developed in the previous section will be used for these two loss situations. Fig. 8 shows the DC/G_{POA} irradiance on the left axis and the change of the same ratio on the right axis as a function of time on January 8, 2012. (a) Data for the same mono-Si systems of Section II are shown unfiltered, (b) using only an outlier filter, and (c) using both an outlier and stability filter. The night before January 8, 2012, about 5 cm of snow fell and covered the modules of the system, while January 8 itself was a cloudless day. Fig. 8 is divided into three different sections; in section 1, the modules are still at least partially covered by snow. As the temperature increased, snow started sliding off the system, increasing the DC/I_{POA} ratio and eventually resulting in a clear system: section 2. However, the snow removal did not occur evenly, and especially just before the modules cleared completely, they showed rapid changes in the DC/G_{POA} ratio (blue crosses).

In Section III-A, decrease in the DC/G_{POA} ratio can again be discerned, but this time, it is because of shading, especially the area highlighted by the green oval. The system's azimuth is 180° south, but the slope on which the system is located does not face due south. Thus, multiple systems are offset by about 40 cm,

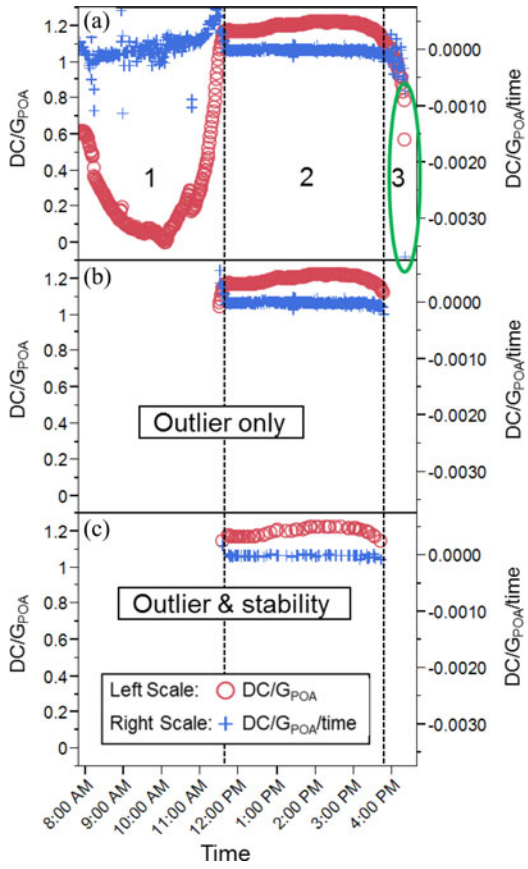

Fig. 8. Ratio dc power over POA irradiance (left axis) and change of that ratio in time (right axis) for a single day on January 8, 2012. (a) Data for the mono-Si systems are shown unfiltered, (b) using only an outlier filter, and (c) both outlier and stability filter.

resulting in the systems shading each other on afternoon winter days. Part (b) shows the same data using only the outlier filter of the DC/G_{POA} ratio where the optimum filter determined by the entire dataset of ten years, and the minimization of the uncertainty was used. The shading situation is completely removed, probably because the shading of the neighboring system is not severe. Most of the data points when snow still covered the system are also removed. However, not all data points just before the system is clear are removed. If a stability filter, using the change of the DC/G_{POA} ratio, is used in addition to the outlier filter (c), a clean dataset may be obtained.

V. Uncertainty Minimization for Systems

The results of the uncertainty minimization methodology, introduced in Section III and applied to three different systems, are shown in Fig. 9. The mono-Si system is the same system as in Section II. Outlier and stability filters were used, as previously discussed. As in Fig. 6, indoor IV measurements are indicated by dashed lines. The uncertainty minimum and the corresponding point on the degradation rate curve are highlighted to guide the eye. The uncertainty minimization method was used directly with the raw datasets. It can be seen that the uncertainty minimum occurs at different points for the different datasets.

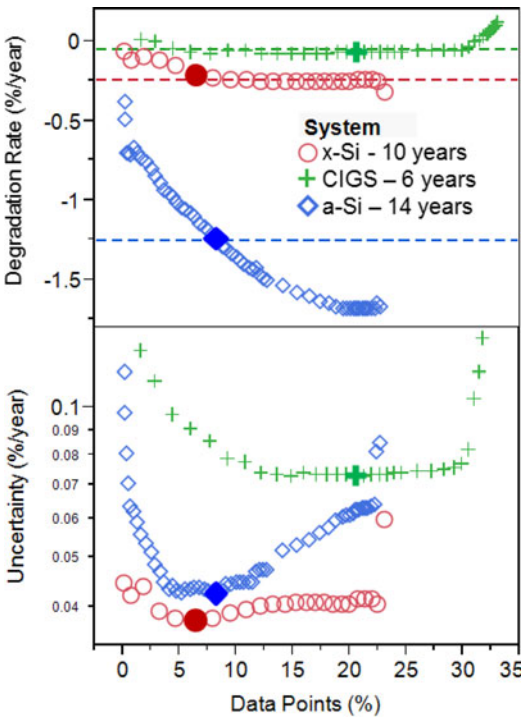

Fig. 9. Degradation rates and uncertainty as a function of percentage of data points left in the dataset for three different systems. Rates determined from indoor IV measurements are indicated by dashed lines. The minimum of the uncertainty curve and the corresponding point on the degradation rate curve are highlighted by a solid symbol.

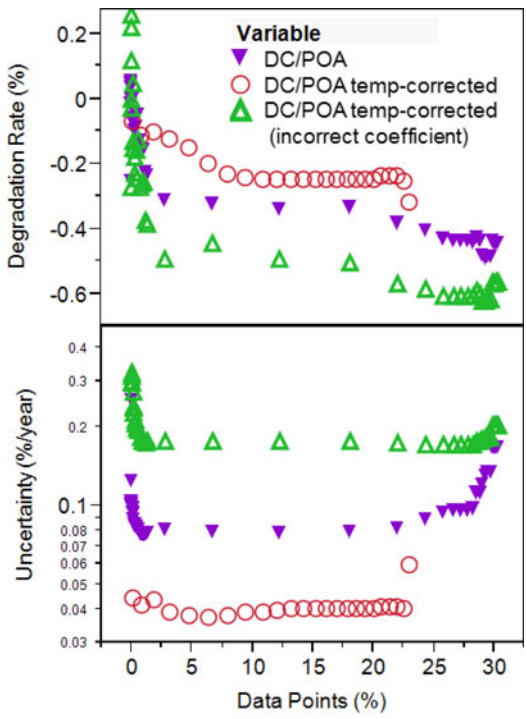

Fig. 10. Degradation rates and uncertainty as a function of percentage of data points left in the dataset for mono-Si system using three different metrics.

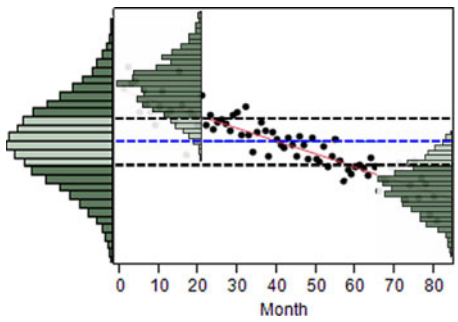

Fig. 11. DC/G_{POA} ratio for a hypothetical dataset with a degradation of –1.3%/year is shown for more than six years. The overall distribution of the filtering parameter DC/G_{POA} is given outside the frame on the left. The inset histograms display the DC/G_{POA} distribution in the first and last month, respectively.

The highest absolute uncertainty corresponds to the dataset with the fewest number of years; however, the corresponding point on the degradation rate curve agrees with the indoor IV measurements. Furthermore, the asymmetry of the uncertainty curve is directly related to the distributions of the filter parameters. If the filter parameter such as the change in module temperature per time were normally distributed and the filtering proceeds in increasing steps around the median of the distribution a symmetric uncertainty curve would result. However, for most datasets most filter parameters are not only not-normally distributed but are most likely correlated. For instance, filtering out the tails of the G_{POA} change per time may not result in removing the tails of DC/G_{POA} distribution. Another interesting feature of Fig. 9 is that the degradation rate curve for the a-Si system displays a significant slope, while similar curves for the other two systems show a more level profile. Figs. 10 and 11 elucidate this particular feature.

Fig. 10 shows degradation rate and uncertainty curve as a function of the percentage of data points left in the dataset for the same mono-Si system of Section II. The temperature-corrected DC/G_{POA} ratio (red circles) is the same as in Fig. 9. The uncorrected DC/G_{POA} ratio (inverted purple triangles) displays not only a higher uncertainty curve than the corrected ratio but the degradation rate curve shows steeper tails than the corrected ratio as well. Finally, a temperature-corrected DC/G_{POA} ratio is shown, but with an incorrect temperature coefficient, resulting in an overcorrection. The overcorrection resulted in a significantly higher uncertainty curve and a substantially smaller plateau on the degradation rate curve. Thus, possible explanations for the steep slope for the a-Si system in Fig. 9 may be with the temperature correction and/or connected with seasonal annealing of the a-Si system.

Fig. 11 illustrates schematically another explanation possibility on a hypothetical dataset. The DC/G_{POA} ratio is shown and assumed to have an overall normal distribution indicated by the histogram outside the frame on the left-hand side. For the sake of simplicity, changes in width and shape of the distribution, as was observed in field observation, has not been taken into account in this simulation [16]. A high degradation of -1.3%/year, similar to the a- Si system in Fig. 9, over more than six years is assumed. The two inset histograms are the DC/G_{POA} distributions in the first and last month, respectively. The overall median is indicated by the blue-dashed line. If a

tight data filtering interval around the median of the DC/G_{POA} ratio is implemented (black-dashed lines), the upper tail in the early months are disproportionally more removed (dark green) than the lower tail. Conversely, the same tight filtering interval leads to a disproportionally larger removal of the lower tail in the later months. Therefore, the remaining data will lead to a much smaller degradation rate. As the overall filtering interval is increased, the degradation quickly increases leading to a fairly high slope in the degradation curve. The situation is exaggerated for clarity purposes.

VI. Elements of a Standard Method

In calculating degradation rates, data filtering plays a very important role but is often neglected. Here, we bring this dark horse out into the light and propose a systematic approach to applying filters, with the goal of defining a consistent way to derive the most accurate degradation rate from a dataset. Such a standardized approach may encompass but is not limited to three distinct sections: 1) data integrity check, 2) data cleaning, and 3) performance analysis.

1) *Data integrity:*
   a) Proceeding directly to the data cleaning or the analysis without proper data integrity check seems intuitive but occurs not infrequently. Simple time series graphs or histograms of the salient analytical parameters often can reveal serious integrity issues such as data shifts. More subtle discontinuities can often be detected through a 12-month moving average. If data shifts are present they can be statistically corrected, as detailed previously [17].
   b) Missing data can be identified easily by a time series graph of the time difference between subsequent data rows: a step that is required in the calculation of the stability filter.
   c) Several strategies exist to address missing data depending on the percentage of data such as replacement with average values or historical values [18], [19].
   d) The same graph can be used to detect changes in data collection frequency. If there is a change in the frequency of data collection, it is useful to equalize the number of points over time.
   e) Sensor redundancy, if present, can be used to detect sensor issues by graphing the mean sensor data versus production data.
   f) Graphing meteorological versus production data in different time increments (weekly, monthly) can often be used in combination with the above checks to detect serious issues with either data.
2) *Data cleaning:*
   a) An outlier filter such as the ratio of power production over irradiance is essential to reduce the effect of undocumented maintenance events: snow or shading.
   b) A stability filter can reduce noise caused by variable days or partial snow covering. It is important that the filter is based on the width of the filter parameter distribution, for instance, the interquartile range.
   c) The minimization of the degradation rate uncertainty may be used to find the best filtering conditions. As different filtering parameters are most likely correlated, simultaneous changing of the individual parameters in increments based on the width of their respective distributions is recommended. If the uncertainty is minimized for each individual parameter successively, stepping through a wider interval simultaneously in order to ascertain that the global minimum was found is recommended.
   d) Finally, filtering for the irradiance of interest can further reduce uncertainty.
3) *Performance analysis:*
   a) Seasonality caused by variables, such as temperature, spectrum, or angle-of-incidence, can have significant impact on long-term field performance. Therefore, corrected metrics such as the temperature-corrected PR are preferred over noncorrected metrics.
   b) Evaluating data only from the same seasonal cycle or using data from the same time of the year may be used to minimize the effects of seasonality, especially for noncorrected metrics.
   c) In addition, a 12-month or 52-week moving average may be used to minimize seasonality.
   d) Varying the temperature coefficient to minimize uncertainty may assist in more accurate degradation rate determination.
   e) The PVUSA regression method uses two regressions: the first to normalize and the second in the time series to assess performance. Most regressions use a standard least square approach based on minimization of the squared residuals making it susceptible to outliers. It may be possible to improve the regression methodology by using for example a robust regression approach based on the minimization of the absolute error.

Acknowledgment

The authors would like to thank the Reliability group at NREL, in addition to E. Maas, K. Luce, H. Groenendaal, and K. Jordan.

References

[1] D. C. Jordan and S. R. Kurtz, "Photovoltaic degradation rates—An analytical review," *Progress Photovoltaics Res. Appl.*, vol. 21, pp. 12–29, 2011.
[2] A. Kimber, T. Dierauf, L. Mitchell, C. Whitaker, T. Townsend, J. Newmiller, D. King, J. Granata, K. Emery, C. Osterwald, D. Myers, B. Marion, A. Pligavko, A. Panchula, T. Levitsky, J. Forbess, and F. Talmud, "Improved test method to verify the power rating of a photovoltaic (PV) project," in *Proc. 34th IEEE Photovoltaic Spec. Conf.*, Philadelphia, PA, USA, 2009, pp. 316–321.
[3] *Standard Test Method for Reporting Photovoltaic Non-Concentrator System Performance*, ASTM E2848–11, 2011.

[4] K. Kiefer, D. Dirnberger, B. Müller, W. Heydenreich, and A. Kröger-Vodde, "A degradation analysis of PV power plants," in *Proc. 25th Eur. Photovoltaic Sol. Energy Conf.*, Valencia, Spain, 2010, pp. 5032–5037.

[5] N. H. Reich, A. Goebel, D. Dirnberger, and K. Kiefer, "System performance analysis and estimation of degradation rates based on 500 years of monitoring data," in *Proc. 38th IEEE Photovoltaics Spec. Conf.*, Austin, TX, USA, 2012, pp. 1551–1555.

[6] J. Adelstein and B. Sekulic, "Performance and reliability of a 1-kW amorphous silicon photovoltaic roofing system," in *Proc. 31st IEEE Photovoltaics Spec. Conf.*, Lake Buena Vista, FL, USA, 2005, pp. 1627–1630.

[7] D. C. Jordan and S. R. Kurtz, "PV degradation Risk," presented at the World Renewable Energy Forum, Denver, CO, USA, May 2012.

[8] H. Haeberlin and Ch. Beutler, "Normalized representation of energy and power for analysis of performance and on-line error detection in PV systems," presented at the 13th Eur. Photovoltaic Sol. Energy Conf., Nice, France, 1995.

[9] C. Jennings, "PV module performance at PG&E," in *Proc. 20th Photovoltaic Spec. Conf.*, Las Vegas, NV, USA, 1988, pp. 1225–1229.

[10] S. Ransome, "Array performance analysis using imperfect or incomplete input data," in *Proc. 23rd Eur. Photovoltaic Solar Energy Conf.*, Valencia, Spain, USA, 2008, pp. 3187–3191.

[11] J. A. del Cueto, "Closed-form solutions and parameterization of the problem of current-voltage performance of polycrystalline photovoltaic modules deployed at fixed latitude tilt," in *Proc. 31st IEEE Photovoltaic Spec. Conf.*, Orlando, FL, USA, 2005, pp. 331–335.

[12] M. A. Quintana, D. L. King, T. J. McMahon, and C. R. Osterwald, "Commonly observed degradation in field-aged PV modules," in *Proc. 29th IEEE Photovoltaic Spec. Conf.*, 2002, pp. 1436–1439.

[13] S. Sakamoto and T. Oshiro, "Field test results on the stability of crystalline silicon photovoltaic modules manufactured in the 1990 s," in *Proc. 3rd World Conf. Photovoltaic Energy Convers.*, Osaka, Japan, 2003, pp. 1888–1891.

[14] K. Morita, T. Inoue, H. Kato, I. Tsuda, and Y. Hishikawa, "Degradation factor analysis of crystalline-Si PV modules through long-term field exposure test," in *Proc. 3rd Conf. Photovoltaic Energy Convers.*, Osaka, Japan, 2003, pp. 1948–1951.

[15] *ISO Guide to the Expression of Uncertainty in Measurement or GUM, 1995. The U.S. edition of the GUM is entitled: American National Standard for Expressing Uncertainty–U.S. Guide to the Expression of Uncertainty in Measurement*, ANSI/NCSL Z540–2–1997.

[16] D. C. Jordan, J. H. Wohlgemuth, and S. R. Kurtz, "Technology and climate trends in PV module degradation," in *Proc. 27th Eur. Photovoltaic Solar Energy Conf.*, Frankfurt, Germany, 2012, pp. 3118–3124.

[17] D. C. Jordan and S. R. Kurtz, "Analytical improvements in PV degradation rate determination," in *Proc. 35th IEEE Photovoltaic Spec. Conf.*, Honolulu, HI, USA, 2010, pp. 2688–2693.

[18] D. C. Jordan, "Degradation rates," presented at the Nat. Renewable Energy Lab. PV Module Rel. Worksh., Golden, CO, USA, Feb. 2010.

[19] Nat. Renewable Energy Lab., Tech. Rep., in press.

Authors' photographs and biographies not available at the time of publication.